Int. J. Electrochem. Sci., 10 **(2015)** 10576 - 10586

International Journal of
ELECTROCHEMICAL
SCIENCE
www.electrochemsci.org

Ni Electrodeposition Enhanced by the Fe Substrate

Jian-Ping Hou[1,2], *Yang Bai*[1,2], *Chang-Wei Su*[1,2,*], *Jun-Ming Guo*[1,2,*]

[1] Key Laboratory of Resource Clean Conversion in Ethnic Regions, Education Department of Yunnan, Yunnan Minzu University, D-306, Guang-Jing Compound, Kunming, 650500, PR China
[2] School of Chemistry and Environment, Yunnan Minzu University, Kunming, Yunnan 650500, PR China
[*]E-mail: abrastein@163.com; guojunming@tsinghua.org.cn

Received: 12 September 2015 / *Accepted:* 9 October 2015 / *Published:* 4 November 2015

Electrodeposition of Ni on 316 stainless steel (ss), Ni/316 ss and Fe/316 ss electrodes was carried out in an acid bath. A Ni deposition peak (C_1) was found between 0.8 and -1.2 V vs. SCE for the two 316 ss and Ni/316 ss electrodes, while two Ni deposition peaks (C_1 and C_2) were clearly observed for the Fe electrode. The C_2 peak occurred at the potential range from -0.7 to -0.85 V, which is more positive than that of the C_1 peak, indicating that Ni deposition was enhanced by the Fe surface. The enhancing effect was firstly found and studied in detail using conventional electrochemical techniques and electrochemical quartz crystal microbalance (EQCM). The results showed Ni deposition was associated with abundant hydrogen evolution at the C_2 peak, and the HER on the Fe surface was also promoted.

Keywords: Electrodeposition; Ni; Fe; Enhancing effect

1. INTRODUCTION

Many researchers considered that the anomalous codeposition of Ni-Fe alloys is resulted from an inhibiting effect of Fe^{2+} ions on Ni deposition [1-5]. However Zech etc [6] found an enhancing effect of Ni^{2+} ions on Fe deposition, which is also contributed to the anomalous behavior. But no one gives a convincing explanation to the anomalous codeposition phenomenon becomes weak along with the Fe content in NiFe alloys. Enhancing effect of the Fe substrate on Ni electrodeposition was firstly found in this paper, probably to be an explanation to the weaker anomalous codeposition for the electrodeposition of Fe-richer NiFe alloys.

The enhancing effect of substrates on metal deposition had been found for many years, for example underportential deposition (UPD) [7-13]. It usually refers to the formation of one monolayer

(very occasionally 2 monolayer) of a metal on a substrate. But the enhancing deposition (ED) of Ni by Fe substrate reported in this paper resulted in forming multilayer Ni, implying that its mechanism is different from that of UPD. An explanation was proposed to understand this different phenomenon in this paper.

In this work, electrodeposition of Ni on the flesh Fe surface was carried out and it was found that the Fe surface enhanced Ni deposition, resulting in two Ni deposition peaks (C_1 and C_2) on the CV. The enhancing effect was studied in detail using conventional electrochemical techniques, scanning electron microscopy (SEM) and electrochemical quartz crystal microbalance (EQCM). A plausible mechanism was proposed to understand the enhancing effect of Fe on Ni deposition.

2. EXPERIMENTAL

Two electroplating baths: A Fe bath: 0.2M $FeSO_4$ + 0.4M H_3BO_3 + 0.5M Na_2SO_4, pH=3.00, and a Ni bath: 0.2M $NiSO_4$ + 0.4M H_3BO_3 + 0.5M Na_2SO_4, pH=3.00. All solutions were prepared with using pure water (16 MΩ cm, prepared by a Molresearc1005a made in Shanghai by Molecular Biotech. Ltd.) and analytical grade reagents. The temperature of all solutions was maintained at 40±0.2 ^oC with a thermostat.

Preparation of Fe/316 ss and Ni/316 ss electrodes: Fe/316 ss and Ni/316 ss electrodes were prepared by electrodeposition of Fe and Ni on the 316 ss electrodes. 316 ss electrodes of dia. 2 mm were polished to a mirror by using waterproof abrasive papers (2000Cw), 3 μm, 1 μm and 0.05 μm alumina powders, then sonicated for 5 min in an ethanol solution (95%), and lastly rinsed thoroughly with pure water. Then Fe or Ni was electrodeposited onto the surface of prepared 316 ss electrode at the potential of -1.2 V vs. SCE for 10s in the Fe or Ni baths. To avoid oxidation, the prepared Fe/316 ss and Ni/316 ss electrodes were used immediately.

Ni deposition on the prepared Fe/316 ss and Ni/316 ss electrodes: Ni deposition behaviors were studied using an electrochemical workstation (IM6eX, Zahner-elektrik GmbH & Co. KG, Germany) with traditional three-electrode cell system. SCE and a helix Pt wire were used as reference and counter electrode, respectively, and Fe/316 ss or Ni/316 ss electrode was used as working electrode.

Cyclic voltammogram (CV) measurements were performed with an a CHI660A electrochemical workstation (CH Instruments Co., USA) [14] at a scanning rate of 20 mV/s, Linear sweep voltammogram (LSV) measurements were performed with an a CHI660A electrochemical workstation (CH Instruments Co., USA) [14] at a scanning rate of 20 mV/s and 100mV/s. Electrochemical quartz crystal microbalance (EQCM): EQCM detection system is composed of a HP4395A impedance analyzer. A Au/PQC (the Au electrode area 0.295cm^2; AT-cut 9MHz Piezoelectric Quartz Crystals) was electrodeposited a layer Fe film at the potential of -1.2 V vs. SCE for 10s to prepare a Fe/Au/PQC electrode, and was then used as work electrode for electrochemically measure in the Ni bath. The SCE and a helix Pt wire were used as reference and counter electrodes, respectively. The EQCM was calibrated for the determination of the proportionality constant (C) between the frequency shift (Δf) and the deposited mass(Δm) [15]:

$$\Delta m = C\Delta f \qquad (1)$$

The value obtained from electrodeposition of Fe from the Fe bath, was C=1.78 ng Hz^{-1}.

SEM: Surface morphology of the obtained deposits was characterized by SEM (KYKY-2800).

3. RESULTS AND DISCUSSION

3.1. Ni enhancing deposition on the Fe surface

The cyclic voltammograms (CVs) of the Fe/316 ss, Ni/316 ss and 316 ss electrodes, recorded in the Ni bath, are shown in Fig. 1 a. Comparing with these CVs, an interesting thing is that two cathodic peaks (C_1 and C_2) are clearly observed on the CV of Fe/316 ss, while only one cathodic peak (C1) occurs on the Ni/316 ss and 316 ss electrodes.

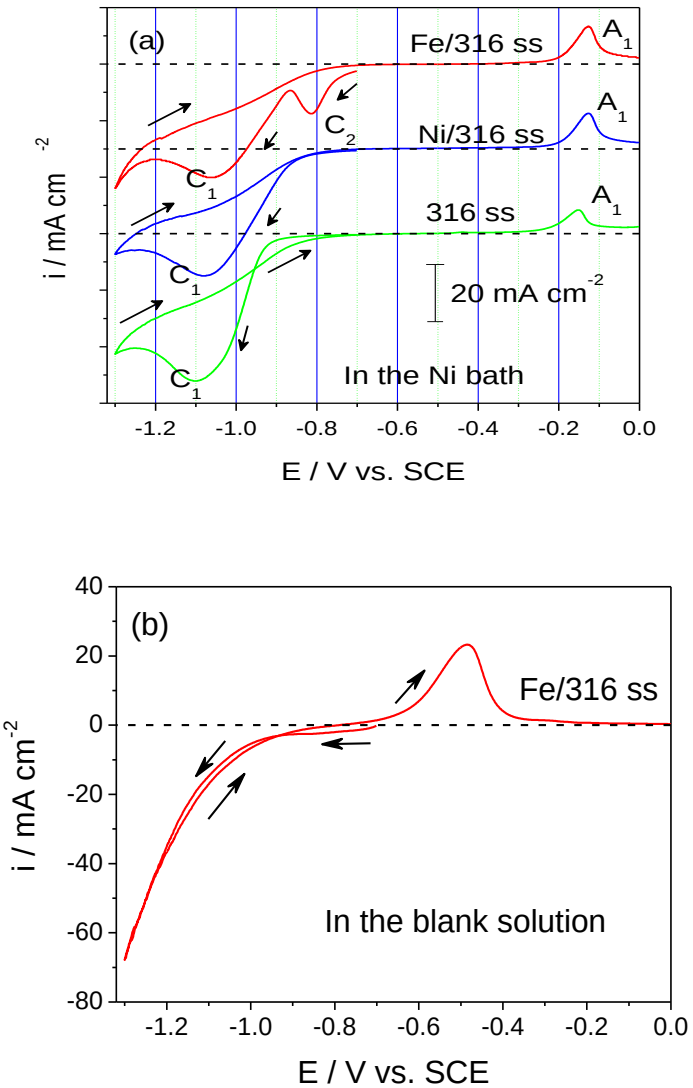

Figure 1. (a) Cyclic voltammograms of the Fe/316 ss, Ni/316 ss and 316 ss electrodes in the Ni bath at a sweep rate of 20 mV/s. The arrows indicate direction of scan voltages. Horizontal dash lines are zero current baselines of respective cyclic voltammograms. (b) A cyclic voltammogram of Fe/316 ss electrode in the blank solution (0.4 MH_3BO_3+0.5 MNa_2SO_4, pH=3.00).

Obviously, the C_1 peak [16] is caused by Ni deposition. What results in the peak C_2? To get to the bottom of this point, the Fe/316 ss electrode was scanned in a blank solution (0.4 M H_3BO_3+0.5 M Na_2SO_4, pH=3.00) and the result is shown in Fig. 1 b. The comparison of these two CVs for the Fe/316 ss between in the Ni bath (Fig. 1 a) and in the blank solution (Fig. 1 b) made us conclude that the C_2 peak is also the contribution of Ni deposition. This phenomenon was also observed in other baths (for example a fluoborate bath or a Watts bath), meaning that anions are of no effect to Ni ED on the Fe surface. However, the potential about Ni ED on the Fe surface is more negative than the Nernst potential corrected for the solution bulk concentration (about -0.5 V vs. SCE).

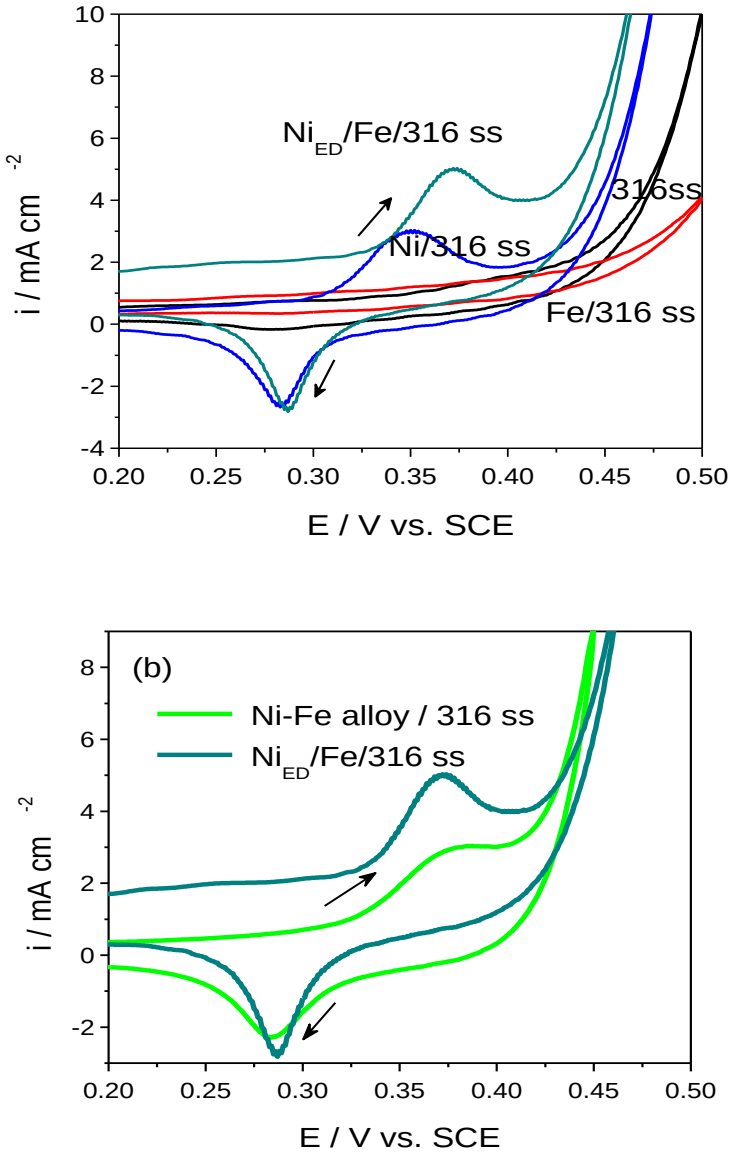

Figure 2. Cyclic voltammograms of (a) Ni_{ED}Fe/316 ss, Ni/316 ss, 316 ss and Fe/316 ss electrodes, (b) Ni_{ED}Fe/316 ss and Ni-Fe alloy/316ss electrodes in 1M NaOH at a sweep rate of 100 mV/s. The Ni-Fe alloy/316ss electrode was prepared at the potential of -1.2 V vs. SCE for 10s in a Ni-Fe bath, which contained 0.1 M $FeSO_4$ + 0.1 M $NiSO_4$+ 0.4 M H_3BO_3 + 0.5 M Na_2SO_4, pH=3.00±0.01.

To further confirm the contribution of Ni deposition to the peak C_2, a label reaction of $Ni(OH)_2$/NiOOH [17, 18] in alkaline solution is used to judge whether there exist Ni deposits on the electrode surface. Firstly, a Fe/316 ss electrode was scanned at the peak C_2 range from -0.7 to -0.85 V at a sweep rate of 20 mV/s in the Ni solution (to prepare Ni_{ED}/Fe/316 ss), then rinsed thoroughly with pure water, lastly transferred into 1M NaOH solution and scanned immediately from 0.2 to 0.5V vs. SCE. The label reaction of $Ni(OH)_2$/NiOOH was observed (see Fig. 2 a), indicating that Ni deposition happened for the peak C_2.

For comparison, CVs of Ni/316 ss, 316 ss and Fe/316 ss electrodes in the 1M NaOH were also shown in the Fig. 2 a. It was noted that the anodic peak of the Ni_{ED}/Fe/316 ss electrode was more positive than that of the Ni/316 ss electrode (Fig.2 a). This shift also occurred on the CV of Ni-Fe alloy/ 316 ss (Fig. 2 b, the similar result was reported by Hu and Wu [19]), implying that a Ni-Fe alloy on the Fe surface should be formed during Ni ED.

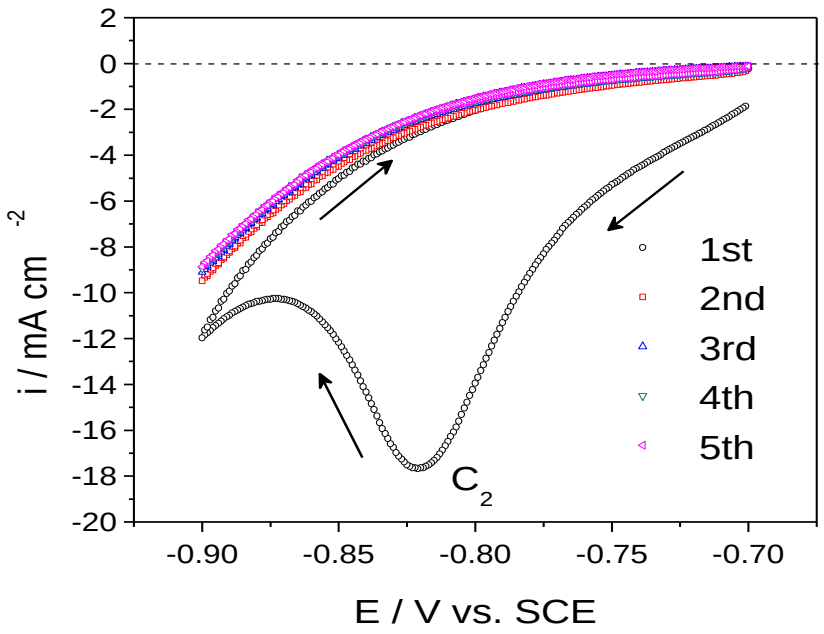

Figure 3. Cyclic voltammograms of a Fe/316 ss electrode with 5 cycles at a sweep rate of 20 mV/s at the peak C_2 range in the Ni bath

But the peak C_2 is impossible to be the contribution of Ni-Fe alloy electrodeposition, Fe^{2+} ions can badly inhibit Ni deposition [1-5] and the deposition potential of Ni-Fe alloy is negative than that of Ni [20]. Therefore, the peak C_2 results from Ni deposition.

Fig. 3 showed CVs of a Fe/316 ss electrode with 5 cycles at a sweep rate of 20 mV/s at the peak C_2 range in the Ni bath. It can be seen that the peak C_2 only appeared in first cycle and in the following cycle, it disappeared. This indicated that the Fe substrate promotes the C_2 peak take place. According to Fig. 3, the total charge of the peak C_2 (Q_{Total}) was calculated approximately to be 100 mC cm^{-2} , which is far larger than that of a monolayer of Ni(111) to be about 0.6 mC cm^{-2} [21-23]. In order to understand this phenomenon, succeeding experiments were performed.

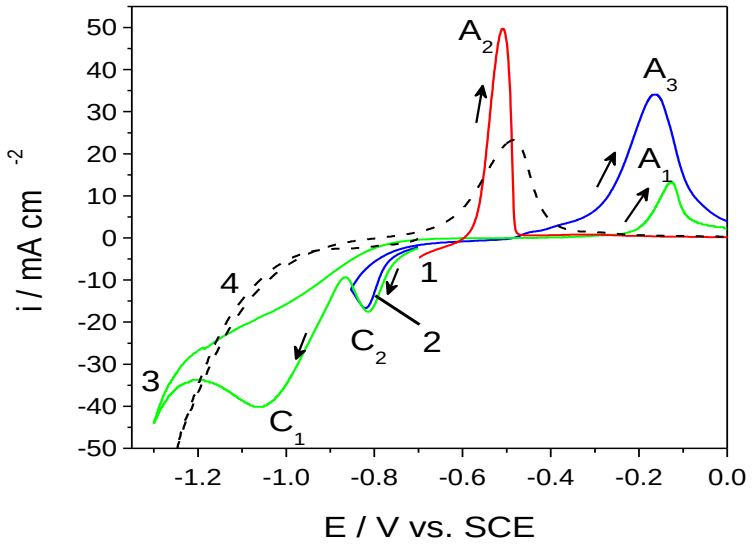

Figure 4. Cyclic voltammograms of the Fe/316 ss with different cathodic switching potentials of -0.7V (curve 1), -0.85V (curve 2) and -1.3V (curve 3) at a sweep rate of 20 mV/s in the Ni bath. Curve 4 is the CV of the Fe/316 ss in the blank solution. The arrows indicate direction of scan voltages.

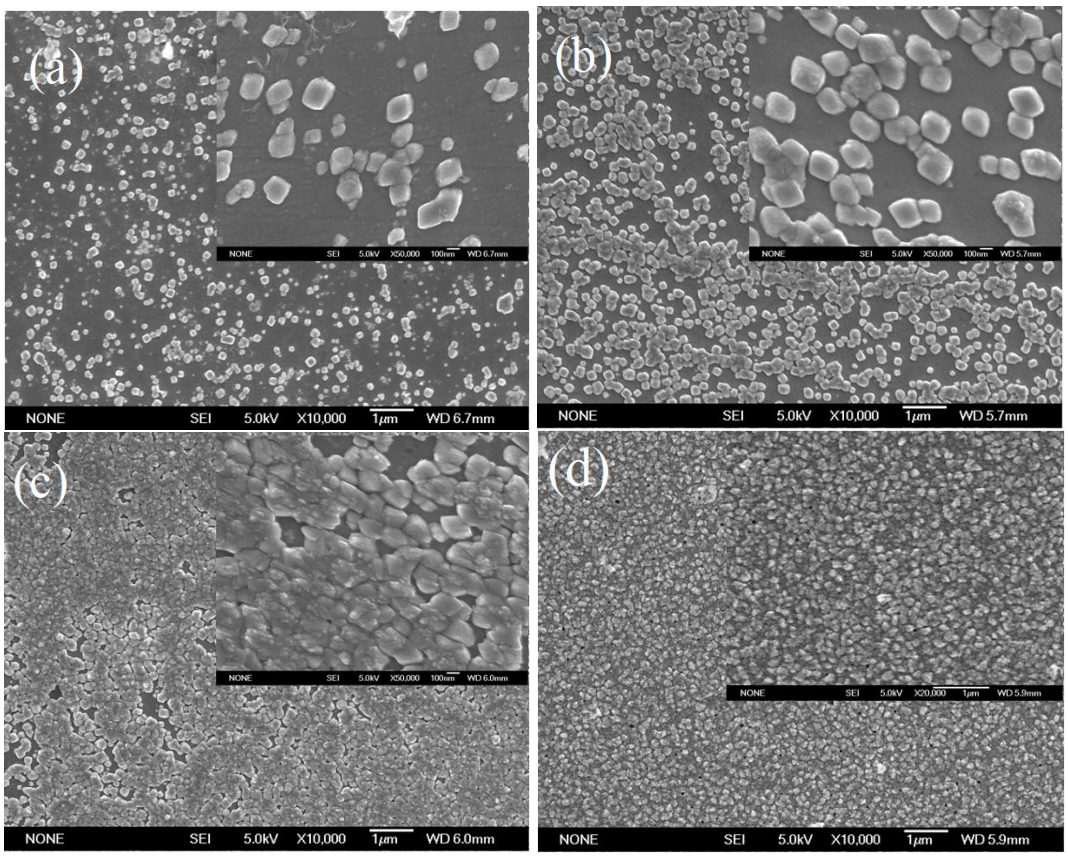

Figure 5. SEM images of Fe/316 ss with different deposition times of (a)5s, (b)10s, (c)100s and (d)1000s

Fig. 4 showed a set of CVs of Fe/316 ss electrode in Ni solution with different cathodic switching potentials of -1.3, -0.85 and -0.7V. For comparison, the CV of Fe/316 ss electrode obtained in a blank solution was also shown in Fig. 4 (curve 4). When the cathodic switching potential (-0.7V) is positive than the onset potential of the peak C_2, no Ni deposition occurred and the anodic peak (A_2, see curve 1) was caused by Fe deposit dissolution. A wider and lower Fe dissolution peak showed in curve 4, probably due to adsorption of hydrogen on the Fe surface in the forward cycle. When the switching potential was moved to -0.85V, Ni ED occurred (see curve 2 in Fig. 4) and an anodic dissolution peak A_3 was observed. In curve 3, the switching potential was moved to -1.3V, Ni normal deposition occurred and only one low anodic peak A_1 observed, and such low anodic current indicated that Ni dissolution was accompanied by passivation. The onset potential of peak A_3 is of positive than A_2 and negative than A_1, implying that an alloy (Ni-Fe) was formed on the surface of Fe during Ni ED.

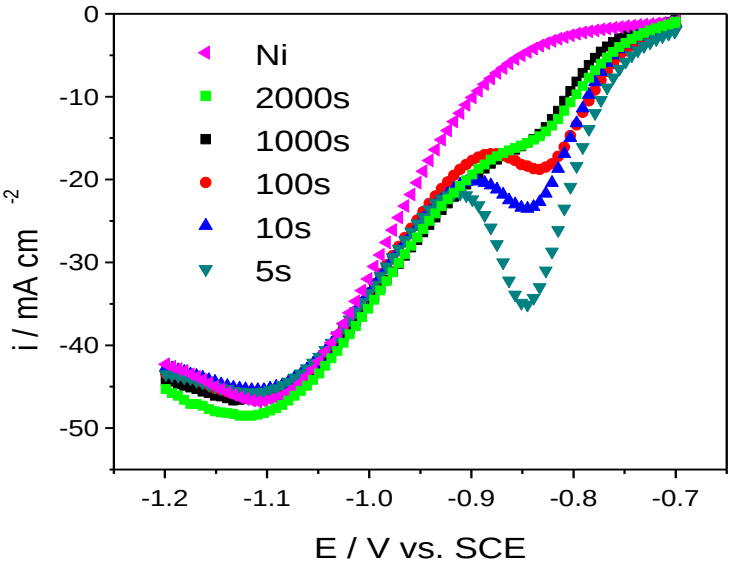

Figure 6. Linear sweep voltammograms of Fe/Ni electrodes in the Ni solution at a sweep rate of 20 mV/s. Fe was electrodeposited on a Ni disk electrode at -1.2V vs. SCE for several seconds (indicated in the figure) in the Fe bath.

The morphology of Fe/316 ss electrodes can badly affect the Ni enhancing deposition. It can be seen from Fig. 5 the Fe crystals exhibit all a cubical structure with tens of nanometers and the number density of Fe nuclei increases with the deposition time. But the peak current of C_2 showed in Fig. 6 decreases with the deposition time of Fe. When the time is over 1000s, the overlap of growing nuclei completely occurred (see Fig. 5 d) and the peak C_2 degenerate to a shoulder. The result indicated that independent Fe nuclei promoted more readily Ni deposition, likely due to their high surface energy resulting in forming NiFe alloy.

An EQCM test was run to eliminate the contribution of HRE to the C_2 peak. A Fe/Au/PQC electrode with 6 cycles was scanned in the peak C_2 potential range at a sweep rate of 20 mV/s in the Ni bath, at the same time the mass changes were recorded by a HP4395A impedance analyzer. The results

were shown in Fig. 7 a and 7 b, respectively. In Fig. 7 a, it can be observed that the charge increment (ΔQ=110mC cm^{-2}) of the first cycle is maximum and for succeeding cycles the ΔQ (about 40mC cm^{-2}) is comparative. Since Ni atomic weight is far bigger than that of H, the data of QCM can be considered to be resulted from Ni deposition.

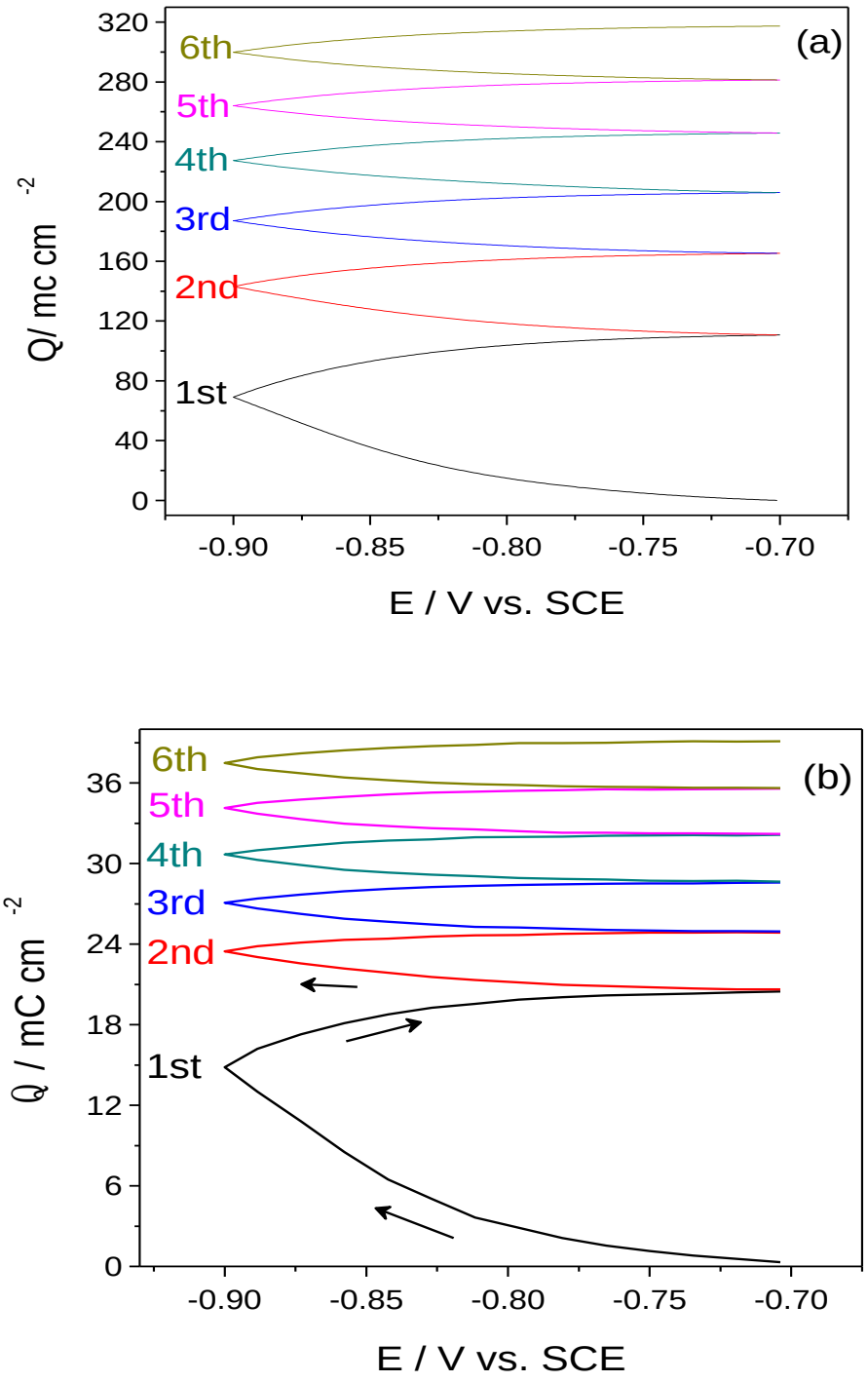

Figure 7. The data obtained by (a) electrochemical workstation and (b) QCM

For the first cycle, the contribution of Ni deposition is only 21mC cm^{-2} (current efficient, CE, equates 19.1%, 35 monolayes Ni), and for other cycles the contribution of Ni deposition is 3.6 mC cm^{-2} (CE=9%, 6 monolayers Ni). The results indicated that the Fe substrate did enhance Ni deposition, but Ni ED is not a main process. The thickness of Ni_{ED} is between 29 and 35 monolayers.

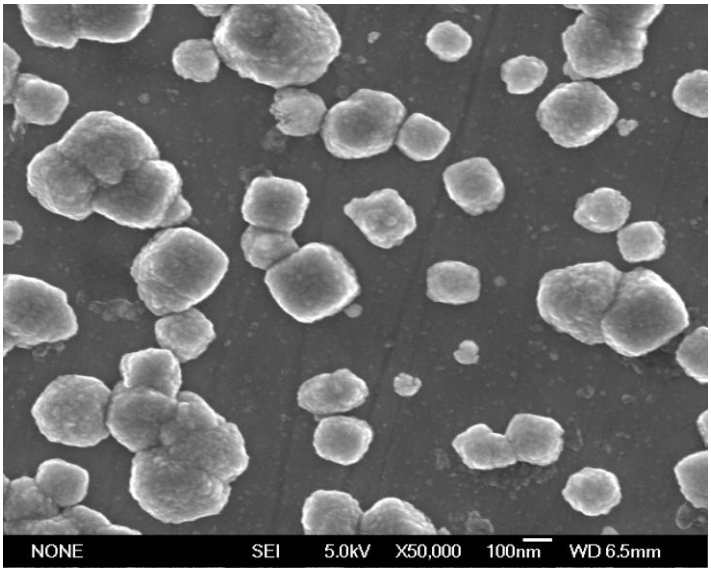

Figure 8. A SEM image of $Ni_{ED}Fe$/316 ss. Ni deposition on the Fe(10s)/316 ss electrode for 100s at the potential of -0.85V

Ni deposited on Fe/316 ss for 100s at the potential of -0.85V vs. SCE in the Ni bath, and its image was shown in the Fig. 8. Compared with the Figure 5 b, it can be clearly observed that Ni deposition mainly occurred on every faces of Fe cubical crystals, that is, the Fe substrate enhanced Ni deposition.

3.2. Explanation of Ni $_{ED}$ on the Fe surface

A two-step reaction mechanism for Ni deposition [24, 25] is widely accepted by researchers. Intermediates (Ni(I) ions) are adsorbed on the electrode surface.

$$Ni(II) + \mathrm{e} \rightarrow Ni(I)_{\mathrm{ads}} \quad (2)$$

$$Ni(I)_{\mathrm{ads}} + e \rightarrow Ni \quad (3)$$

A hydrated Ni^{2+} ion involves four water molecules, and in acid solutions it may be undergo following reduction processes on the Fe surface.

$$\left[Ni(H_2O)_4\right]^{2+} / Fe + 5\mathrm{e} \rightarrow Ni(I)_{\mathrm{ads}} \bullet 4OH^- / Fe + 2H_2 \quad (4)$$

$$Ni(I)_{\mathrm{ads}} \bullet 4OH^- / Fe + 4H^+ + 5\mathrm{e} \rightarrow Ni - Fe + 2H_2 + 4OH^- \quad (5)$$

And the total electrochemical reaction is,

$$[Ni(H_2O)_4]^{2+} / Fe + 4H^+ + 10\mathrm{e} \rightarrow Ni - Fe + 4H_2 + 4OH^- \quad (6)$$

From this reaction it can be calculated that the current efficient is 20%, which is consistent with the data(19.1%) obtained by EQCM.

Fe and Fe-rich Fe-Ni alloys electrodeposited are all body-centered cubic (BCC) structures [26-28] with low density, so neonatal Ni atoms with high energy likely diffuse into the BCC crystals, forming face-centered cubic crystals. Hence, Ni deposition more than monolayer occurred on the Fe substrate.

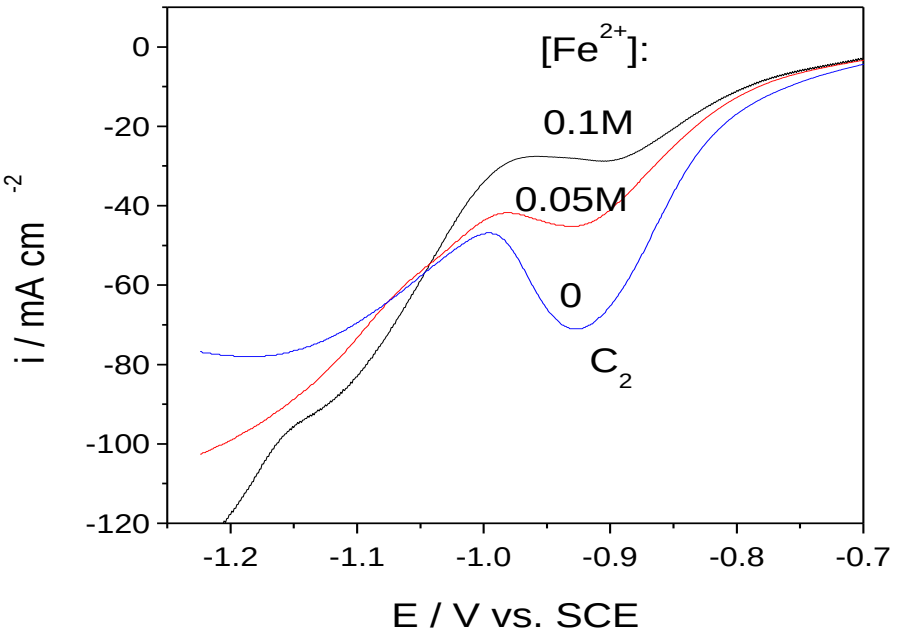

Figure 9. The effect of Fe^{2+} ions on Ni ED, sweep rate: 100 mV/s,

It is well known that the nickel deposition is inhibited by Fe^{2+} ions [1-5]. The inhibition effect of Fe^{2+} ions on the Ni ED is also observed (see Fig. 9). Since Fe^{2+} ions are impossible to be electrochemical reduced at the potential range of the peak C_2, Fe^{2+} ions probably integrate with OH^- ions to form $Fe(OH)_2$ adsorption ions on the electrode, consequently suppressing the electrochemical reaction (5). Maybe, anomalous codeposition of nickel-iron alloys is partially resulted from the adsorption of $Fe(OH)_2$.

$$Fe^{2+} + 2OH^- \rightarrow Fe(OH)_{2,ads} \quad (7)$$

4. CONCLUSION

The Fe substrate enhances Ni deposition and more HRE. Ni fresh atoms reduced possibly diffuse into the Fe substrate, consequently multilayer (between 29 and 35) Ni deposited. A plausible mechanism of Ni ED on the Fe surface was proposed to explain the enhancing effect of Fe.

ACKNOWLEDGEMENTS
This work was financially supported by the National Natural Science Foundation of China (51561032, 51262031, 51462036), Program for Innovative Research Team (in Science and Technology) in University of Yunnan Province (2011UY09), Yunnan Provincial Innovation Team (2011HC008), and Innovation Program of Yunnan Minzu University (2015YJCXY282, 2015TX06).

References

1. A. Brenner, *Electrodeposition of Alloys,* Academic Press, Inc., New York, (1963).
2. H. Li, F. Ebrahimi, *Mater. Sci. Eng. A*, 347 (2003) 93.
3. Katalin Neuróhr, Attila Csik, Kálmán Vad, Györgi Molnár, Imre Bakonyi, László Péter, *Electrochim. Acta,* 103 (2013) 179– 187.
4. Isao Matsui, HirokiMori, Tomo Kawakatsu, Yorinobu Takigawa, Tokuteru Uesugi, Kenji Higashi, *Mater. Sci. Eng. A,* 607 (2014) 505–510.
5. R. S. Larson, *J. Electrochem. Soc.*, 154 (2007) D427.
6. N. Zech, E. J. Podlaha, D. Landolt, *J. Electrochem. Soc.*, 146 (1999) 2892.
7. M. Palomar-Pardavé, E. Garfias-García, M. Romero-Romo, M.T. Ramírez-Silva, N. Batina, *Electrochim. Acta,* 56 (2011) 10083– 10092.
8. J. Aldana-González, J. Olvera-García, M.G.Montes de Oca, M. Romero-Romo, M.T. Ramírez-Silva, M. Palomar-Pardavé, *Electrochem. Commun.,* 56 (2015) 70–74.
9. J.-W. Yan, J.-M. Wu, Q. Wu, Z.-X. Xie, and B.-W. Mao, *Langmuir*, 19 (2003) 7948.
10. M. Chatenet, R. Faure, Y. Soldo-Olivier, *J. Electroanal. Chem.*, 580 (2005) 275.
11. M. Chatenet, Y. Soldo-Olivier, E. Chainet, R. Faure, *Electrochem. Commun*., 9 (2007) 1463.
12. C.A. Paddon, and R.G. Compton, *J. Phys. Chem. C*, 111 (2007) 9016.
13. A. Milchev, Russ. *J. Electrochem*., 44 (2008) 619.
14. Y. Zhang, M. Liu, M. Wang, Q. Xie, S. Yao, *Sens. Actuators B*, 123 (2007) 444.
15. G. Z. Sauerbrey, *Phys.*, 155 (1959) 206.
16. A. Ispas, H. Matsushima, A. Bund, B.J. Bozzini, *J. Electroanal. Chem.,* 626 (2009) 174.
17. M. A. Sattar, B. E. Conway, *Electrochim. Acta,* 14 (1969) 695.
18. F. Paloukis, S. Zafeiratos, V. Drakopoulos, S. G. Neophytides, *Electrochim. Acta,* 53 (2008) 8015.
19. C. C.Hu, Y. R. Wu, *Mater. Chem. Phys.*, 82 (2003) 588.
20. C. -W. Su, F. -J. He, H. Ju, Y. -B. Zhang, E.-L. Wang, *Electrochim. Acta*, 54 (2009) 6257.
21. F. A. Moller, J. Kintrup, A. Lachenwitzer, O.M. Magnussen, R. Behm, *J. Phys. Rev. B*, 56 (1997) 12506.
22. S. Morin, A. Lachenwitzer, F.A. Moller, O.M. Magnussen, R. Behm, *J. Electrochem. Soc.*, 146 (1999) 1013.
23. A. Vaskevich, F. Sinapi, Z. Mekhalif, J. Delhalle, I. Rubinstein, *J. Electrochem. Soc*., 152 (2005), C744.
24. W. G. Proud, C. Muller, *Electrochim. Acta,* 38 (1993) 405.
25. E. Epelboin, M. Joussellin, R. Wiart, *J. Electroanal. Chem.*, 101 (1979) *281.*
26. I. Tabakovic, V. Inturi, J. Thurn, M. Kief, *Electrochim. Acta,* 55 (2010) 6749.
27. C. -W. Su, E.-L. Wang, Y. -B. Zhang, F. -J. He, *J. Alloys Compd.*, 474 (2009) 190.
28. S. D. Leith, S. Ramli, D. T. Schwartz, *J. Electrochem. Soc.*, 146 (1999) 1431.